Turkish Journal of Electrical Engineering & Computer Sciences

http://journals.tubitak.gov.tr/elektrik/

Research Article

Turk J Elec Eng & Comp Sci
(2019) 27: 120 – 138

doi:10.3906/elk-1802-144

Three-channel control architecture for multilateral teleoperation under time delay

Uğur TÜMERDEM*
Department of Mechanical Engineering, Faculty of Engineering, Marmara University, Istanbul, Turkey

Received: 18.02.2018 • **Accepted/Published Online:** 07.09.2018 • **Final Version:** 22.01.2019

Abstract: Multilateral teleoperation is an extension of bilateral/haptic teleoperation framework to multiple operators/robots and finds applications in haptic training. As in bilateral teleoperation, time delay is an important problem, and stability and transparency, which quantifies the performance of the teleoperation system, are critical in the design of multilateral control systems. This paper proposes a novel three-channel-based multilateral control architecture with damping injection to guarantee delay-independent L_2 stability and high transparency in multilateral teleoperation systems. The theoretical and computational analyses are verified with experiment results.

Key words: Robotics, teleoperation, haptics, time delay

1. Introduction

Multilateral teleoperation systems are multirobot extensions of bilateral teleoperation systems. In bilateral teleoperation, an operator manipulates a master robot to control the motion of a slave robot with force feedback from the slave. In multilateral teleoperation, multiple operators can control a single slave robot or multiple slave robots with force feedback. With the advances in communication technologies and widespread use of bilateral teleoperation systems in applications such as robotic surgery [1], robotic rehabilitation [2], and telediagnosis [3], multilateral teleoperation systems have also started drawing attention as they can be used in training operators for bilateral teleoperation. Since force information is often transmitted among the robots in multilateral teleoperation, one master can use his/her force input to train a novice operator during a teleoperation task. Due to the existence of multiple robots in an arbitrary multilateral teleoperation setup, designing controllers that can guarantee stability and good kinesthetic performance is a difficult problem compared with bilateral teleoperation.

Even in bilateral teleoperation, stability and transparency are important problems when time delays exist on the communication channels among the robots. In bilateral teleoperation, it was first shown that stability under time delay can be guaranteed through the passivity of the interconnected control system [4]. It was shown that control system performance can be measured by the transparency/hybrid matrix which gives the relationship between master velocity and force signals in frequency domain [5]. Transparency can be achieved in bilateral teleoperation by the use of Lawrence four-channel architecture which makes use of four communication channels among the master and slave robots: position measurements are exchanged among the robots with two channels and force measurements are also exchanged with two other channels adding up to a total of four channels [6]. These measurements are used in the master and slave controllers, and as a result, the control

*Correspondence: ugur.tumerdem@marmara.edu.tr

systems are strongly coupled. Due to this strong coupling, it was also shown in [6] that four-channel controllers are unstable under time delay and cannot provide good transparency. On the other hand, two-channel-based passivity controllers can guarantee stability under time delay but they cannot achieve high transparency. It was shown in [6] that there is a trade-off between stability and transparency under time delay. Robust control theory can be used to achieve this trade-off in the presence of time delay [7] but robust control approaches can often result in complex controllers. In [8] and [9], it was shown that using local force feedback and utilizing three instead of four channels (two for position and one for force), it is possible to get high transparency under time delay, but stability is dependent on the environmental and operator impedance parameters and cannot always be guaranteed. On the other hand, a damping injection method was introduced as a trade-off between transparency and stability in four-channel teleoperation by imposing a small gain condition on the interconnection [10]. With this method, the system response is slowed down due to damping injection but steady-state errorless position tracking and force reflection can be achieved.

The name "multilateral teleoperation" has been used in the literature to refer to different kinds of multirobot teleoperation. In [11], a classification of the types of multilateral teleoperation was provided. According to this classification, multilateral teleoperation in this paper implies dual-user–shared control, or multiuser-shared control systems. In multilateral teleoperation, first controllers were developed by extending the four-channel architecture to multiple robots [12]. In multilateral teleoperation, a four-channel control architecture implies that all robots share their force and position measurements among themselves. In effect, they can be considered $n \times 4$-channel controllers where n is the number of robots. Sometimes communication among the master robots is omitted, for instance, a two-channel force–position-based robust multilateral control architecture was proposed in [13]. In this architecture, two master robots communicate with the slave only and receive slave position measurements and the slave robot receives master force measurements. A method based on n-port passivity for determining the stability of multilateral teleoperation systems was presented in [14] and [15]. Also, in [16] and [17], passivity was used to guarantee stability of multilateral teleoperation systems using the two-channel communication architecture, meaning that only two measurements are exchanged among the robots. In [16], a controller that transmits wave variables among the robots with two communication channels was proposed, guaranteeing the passivity of the system, and in [17], a time domain passivity observer was utilized on a two-channel control architecture similar to that in [13] but both of the systems suffer from steady-state errors due to passivity constraints. In [18], a position–position-based consensus algorithm was proposed for shared interaction on a virtual environment that can guarantee passivity. In [19], a wave-variable-based system was proposed for a multimaster single-slave system, but this method also has large steady-state error. In [20], an adaptive controller was proposed to guarantee nonlinear stability of a two-master two-slave system but this method has not been applied to a multilateral haptic training scenario. In [21], a position–position-based algorithm with damping injection was proposed for a dual-master single-slave system guaranteeing stability in the sense of Lyapunov. However, the results demonstrated that the system has large positioning and force reflection errors. To get better performance and still guarantee stability, for trilateral teleoperation (two masters and one slave), a less conservative stability criterion was proposed in [22] and [23]: absolute stability for the two-channel PP architecture. Although this criterion can be used to choose different controller gains for each robot, it does not solve the steady-state error problem. The stability conditions can be relaxed further by taking environmental/operator parameters into consideration [24]. A delay-independent L_2 small-gain theorem was proposed in [25] for guaranteeing stability by taking environmental parameters into consideration along with

a four-channel-based architecture with damping injection to eliminate steady-state errors. However, it can be shown that the transparency of the system is not ideal when there is time delay on the communication channels.

There still exists a need for a multilateral control system that can achieve better transparency under time delay while guaranteeing stability. In this paper, the three-channel architecture in [8] is extended to multilateral teleoperation. Furthermore, by proposing a scalable L_2 stability analysis method for this architecture and introducing damping injection, delay-independent stability of the three-channel multilateral control architecture is guaranteed. This paper focuses on the application to trilateral haptic training systems which typically are dual-user single-slave systems. However, the method can easily be scaled to N robot systems. The claims of the paper were verified with analytical stability and transparency comparisons as well as experiment results.

The contributions of the paper can be summarized as follows: 1- Three-channel architecture is extended to multilateral systems, 2- Three-channel controllers are modified with damping injection to guarantee delay-independent stability of three-channel multilateral systems under constant time delay, 3- Delay-independent L_2 input–output stability analysis for three-channel-based multilateral teleoperation systems is proposed, 4- The use of inverse hybrid matrices is proposed to compare the transparency of the proposed three-channel controllers with some of the existing controllers under constant time delay.

The paper is organized as follows: in Section 2, the theory of multilateral teleoperation is explained, conventional and proposed multilateral teleoperation architectures are discussed. In Section 3, stability analysis of the proposed architecture under time delay is presented. In Section 4, the transparency of the proposed method is demonstrated and compared with existing architectures in the literature. In Section 5, experiment results comparing the proposed method with conventional methods are provided. Section 6 concludes the paper.

2. Multilateral teleoperation

In multilateral teleoperation, teleoperation is performed through haptic agreement among multiple operators. This can be especially useful in a cooperative teleoperation scenario or in haptic training for teleoperation. Haptic training can have applications in robotic surgery, driver/pilot training, aircraft/vehicle simulators, or any system utilizing teleoperation. In most haptic training scenarios, trilateral teleoperation would be adequate as there would be need for two master robots and operators, one being the instructor and the other being the trainee, and one slave robot to be operated.

For multilateral teleoperation, the basic setup that is assumed throughout this paper can be seen in Figure 1a; there are two master robots, linear motors in their simplest form whose shafts are moved independently by their respective master operators through the application of force, and there is an identical slave robot which will perform a motion that is the result of the agreement among masters. The goal in multilateral haptic training can also be seen in Figure 1b from the equivalent physical representation of the trilateral system. Although the master operators control separate master motor shafts, ideally, they should feel like they are holding a single shaft, the slave shaft, and be able to manipulate it together. The operators should also be able to feel the forces applied on the shaft by the other operator as well as the environment. Obviously, the robots in a given teleoperation scenario are spatially separated from each other. Thus, this rigid mechanical coupling should be realized by a distributed-network-based controller. The physical task in this case should be transformed into control system performance goals: the masters should feel like moving the same shaft without any slip, and the forces applied by the environment and the other master should be transmitted to them exactly. The first goal can be achieved by making sure that each robot is tracking the same trajectory at any given time, and the second goal can be described by the law of action and reaction: the sum of all the forces acting on the robot

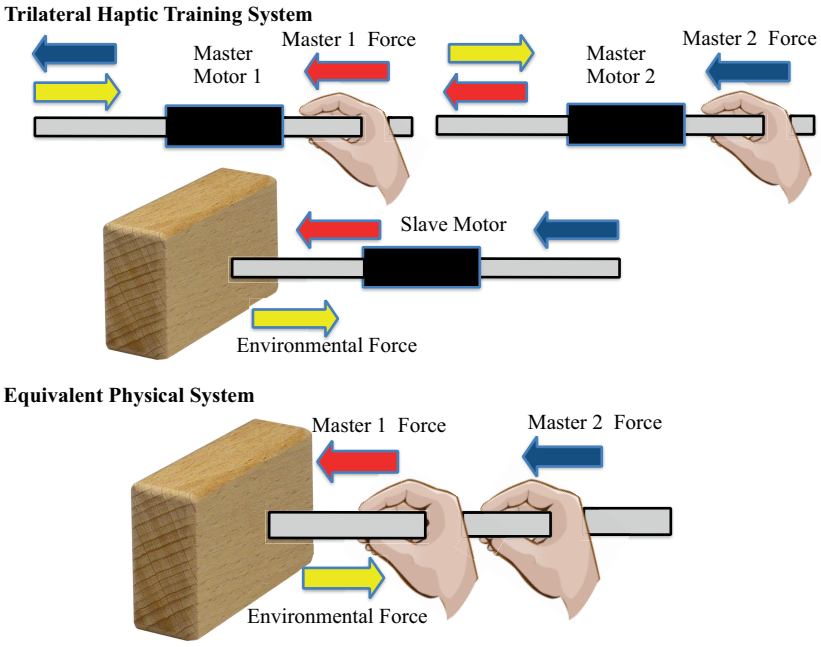

Figure 1. Trilateral haptic training system with linear motors and equivalent physical representation.

shafts should always be equal to zero. These control system goals can be mathematically summarized as [12]:

$$F_{m1}(t) + F_{m2}(t) + F_s(t) = 0, \tag{1}$$

$$x_{m1}(t) = x_{m2}(t) = x_s(t), \tag{2}$$

where $F_{m1}(t)$, $F_{m2}(t)$, and $F_s(t)$ are scalar force measurements from the masters and the slave, and x_{m1}, x_{m2}, and x_s are the position measurements of each robot, and t is time. To achieve these control goals, Lawrence architecture [6, 8] can be used to design multilateral controllers.

Figure 2 shows the block diagram representation of a multilateral system with three robots (trilateral) using a modified Lawrence architecture. In this architecture, channels are used to represent the signal flow among the robots. Two-, three-, or four-channel controllers can be represented with appropriate choice of Lawrence channel parameters. Dynamics of each robot together with the control input can be written in frequency domain as:

$$Z_{mi} v_{mi} = F_{mi} + F_{ci}, \tag{3}$$

$$Z_s v_s = F_{cs} - F_s, \tag{4}$$

where i denotes the number of the master, $Z_{mi} = m_{mi}s$ and $Z_s = m_s s$ are the master and slave robot impedances which are motor shafts masses, v_{mi} and v_s are the master and slave velocities, F_{mi} and F_s are the master and slave force inputs from the operators and environment, F_{ci} and F_{cs} are the master and slave robot control inputs. Here, the human and environment are represented by the following linear time invariant (LTI) dynamics:

$$F_{m1} = F^*_{h1} - Z_{h1} v_{m1}, \tag{5}$$

$$F_{m2} = F^*_{h2} - Z_{h2} v_{m2}, \tag{6}$$

$$F_s = F^*_e + Z_e v_s, \tag{7}$$

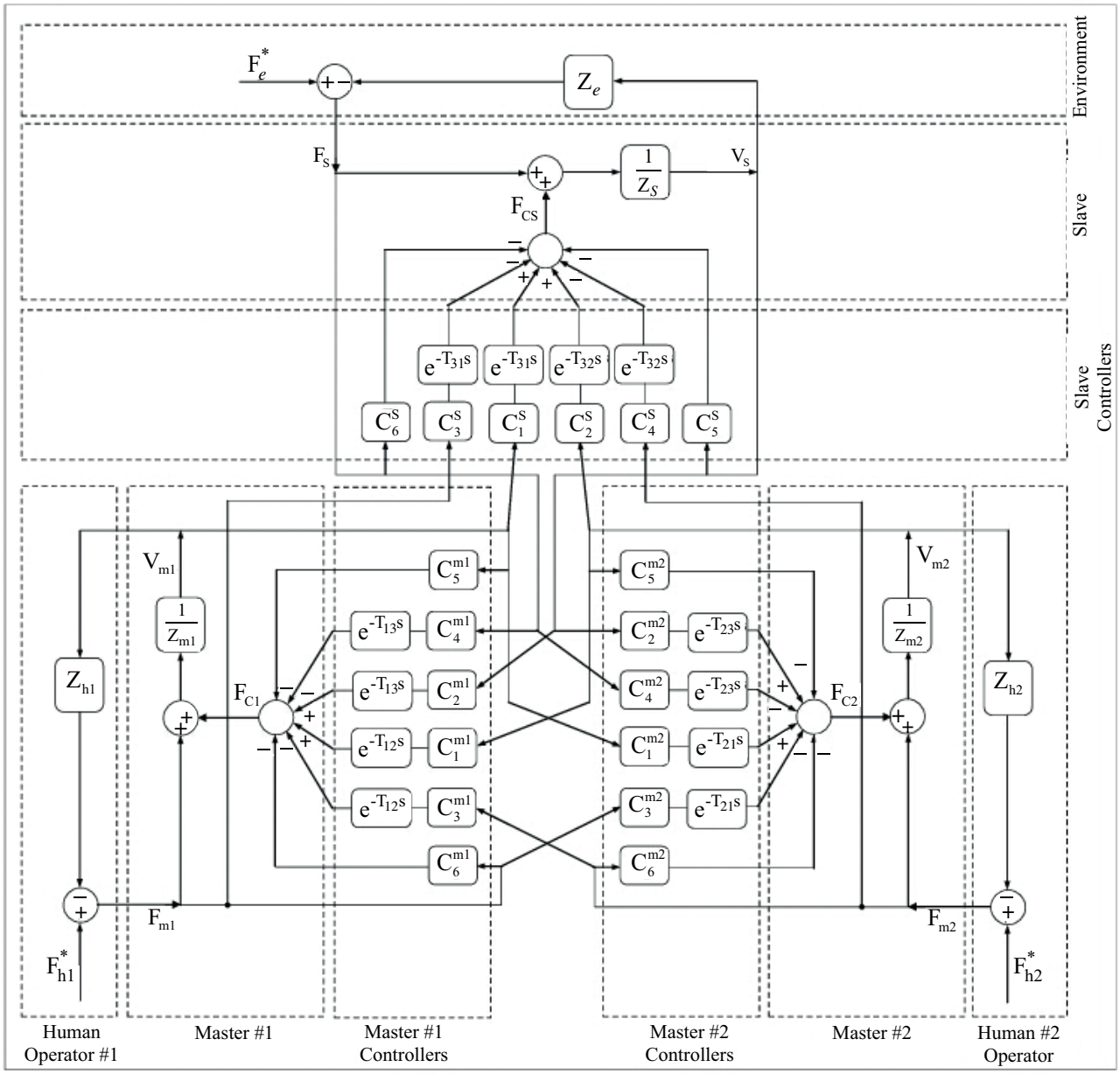

Figure 2. Lawrence architecture for trilateral teleoperation.

where Z_{hi} are the human impedances where the subscript i identifies the master, Z_e is the environment impedance, and F^*_{h1}, F^*_{h2}, and F^*_e are the exogenous force inputs by the masters and the environment which are independent of the states of the teleoperation system. Also, environment and human impedances can be modelled as:

$$Z_{hi} = \frac{k_{zmi}}{s} + b_{zmi} + m_{zmi}s, \tag{8}$$

$$Z_e = \frac{k_{ze}}{s} + b_{ze} + m_{ze}s, \tag{9}$$

which are LTI mass-spring-damper models. According to the modified Lawrence architecture in Figure 2, any Lawrence-architecture multilateral controller can be written as:

$$F_{c1} = -C_5^{m_1} v_{m_1} - C_4^{m_1} e^{-T_{13}s} F_s + C_2^{m_1} e^{-T_{13}s} v_s + C_1^{m_1} e^{-T_{12}s} v_{m_2} + C_3^{m_1} e^{-T_{12}s} F_{m_2} - C_6^{m_1} F_{m_1}, \tag{10}$$

$$F_{c2} = -C_5^{m_2} v_{m_2} - C_4^{m_2} e^{-T_{23}s} F_s + C_2^{m_2} e^{-T_{23}s} v_s + C_1^{m_2} e^{-T_{21}s} v_{m_1} + C_3^{m_2} e^{-T_{21}s} F_{m_1} - C_6^{m_2} F_{m_2}, \tag{11}$$

$$F_{cs} = -C_5^{s} v_s + C_4^{s} e^{-T_{32}s} F_{m_2} + C_2^{s} e^{-T_{32}s} v_{m2} + C_1^{s} e^{-T_{31}s} v_{m_1} + C_3^{s} e^{-T_{31}s} F_{m_1} + C_6^{s} F_s, \tag{12}$$

where C_5 terms are local position controllers, C_6 terms are local force compensators, C_1 and C_2 are position/velocity (used interchangeably) channel transfer functions among the robots, C_3 and C_4 are the force channel transfer functions/feedback compensators among the robots, and $e^{-T_{ij}s}$ are the time delays on the channels from robot j to robot i. For four-channel teleoperation, these values are typically chosen as [12]:

$$C_1 = C_2 = \frac{C_5}{2} = \frac{C_p}{s} = \frac{k_p}{s} + k_v, \tag{13}$$

$$C_3 = C_4 = 1, \tag{14}$$

$$C_6 = 0, \tag{15}$$

where $C_p = k_p + k_v s$ is a PD position controller with the PD coefficients k_p and k_v. Although this architecture is capable of achieving transparency in the absence of time delays, it was shown in [25] that it cannot preserve the stability or the transparency of the teleoperation system under time delays. A two-channel position–position (PP) controller was proposed in [23] and [26] for guaranteeing absolute stability/passivity of the system under time delays. However, this two-channel architecture is not transparent: the controller has large steady-state errors and low-force reflection bandwidth. Figure 3a shows four-channel, and Figure 3b shows two-channel PP architecture information flows for trilateral teleoperation. In the figure, M_1, M_2, and S nodes represent masters 1 and 2 and slave robots, respectively, and X and F values are the transmitted position and force values among robots.

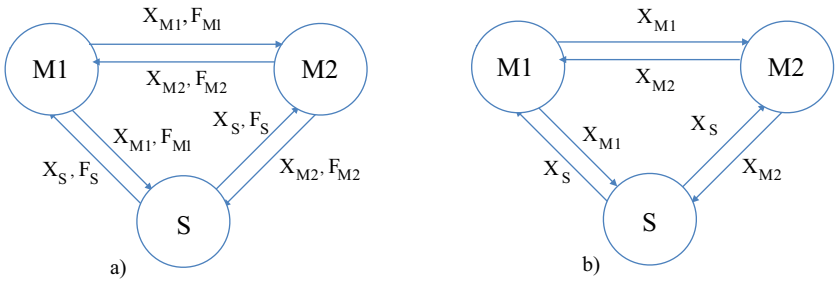

Figure 3. Information flow in 4-channel- and 2-channel-based architectures.

As a solution, a modification to the four-channel algorithm was proposed in [25] by changing the position controllers as follows:

$$C_1 = C_2 = \frac{C_p}{s} = \frac{k_p}{s} + k_v, \tag{16}$$

$$C_5 = \frac{2C_p}{s} + b, \tag{17}$$

where the channel position controllers C_p are PD controllers and the local controllers are selected as PD+D controllers with additional local damping injection terms b to stabilize the system. It was shown that the transparency and stability are improved with this controller.

In this paper, it is shown that the four-channel architecture with damping injection is not ideal in terms of transparency under time delay. By utilizing the idea proposed in [8] for bilateral teleoperation, a novel three-channel control architecture for multilateral teleoperation systems is proposed. In [8], it was shown that the use of three-channel architecture is equivalent to the four-channel controller in terms of transparency under no time delay, but unlike the four-channel architecture, it can achieve delayed transparency under time delay. With transparency analyses, it was shown that the multilateral three-channel architecture is also superior to two-channel and four-channel architectures in multilateral teleoperation. In [8], the authors also provided the environmental conditions under which the bilateral system would be stable. In this paper, it was also shown, with the inclusion of damping injection, that the stability of a three-channel control system (bilateral or multilateral) can be guaranteed for different environmental parameters.

The idea in three-channel bilateral teleoperation is to compensate the effect of the external forces acting on a given robot (master or slave) by using local force feedback channels, and realizing pure position control on one of the robots. Thus, position information is sent from one robot to the position-controlled robot, and the position-controlled robot sends both force and position information to the other robot. The position-controlled robot can either be the master or the slave. In the case of multilateral or even trilateral teleoperation, due to the number of robots and possible communication strategies, there are multiple combinations that could be called three-channel architectures.

Figure 4 shows the feasible ones. Figures 4a–4c show a class of controllers that is termed the 2FP1P architecture, in which one robot is position-controlled and the other two robots are position/force-controlled. In Figures 4a–4c, the cases where the position-controlled robot is the slave, master 2, and master 1, respectively, are shown. Figures 4d–4f show the 2P1FPa class where two robots are position-controlled and the third robot is force/position-controlled. Figures 4d–4f also show the cases where the force/position controlled robot is the slave, master 1, and master 2, respectively. Note that in both of these classes, all the robots communicate with each other. The third class presented is called 2P1FPb. Here, two robots are position-controlled, and the third one is position/force-controlled, but the difference is that the position controlled robots do not communicate with each other, they communicate only with the third robot. Among these, only 2P1FPb enables a simple decomposition into input–output form that yields a solution for stability under time delay. Therefore, this paper will be focusing on the 2P1FPb architecture, and the information flow in Figure 4g will be chosen without loss of generality, which assumes that the slave robot is position/force-controlled and masters are position-controlled. This proposed architecture has the following channel selections with damping injection in the case of trilateral teleoperation:

$$C_1^s = C_2^s = C_2^{m_1} = C_2^{m_2} = \frac{C_p}{s} = \frac{k_p}{s} + k_v, \tag{18}$$

$$C_5^s = \frac{2C_p}{s} + b_s, C_5^{m_1} = \frac{C_p}{s} + b_{m1}, C_5^{m_2} = \frac{C_p}{s} + b_{m2}, \tag{19}$$

$$C_1^{m_1} = C_1^{m_2} = 0, \tag{20}$$

$$C_6^s = 0, C_6^{m_1} = C_6^{m_2} = 1, \tag{21}$$

$$C_3^s = C_4^s = 1, C_3^{m_1} = C_3^{m_2} = C_4^{m_1} = C_4^{m_2} = 0. \tag{22}$$

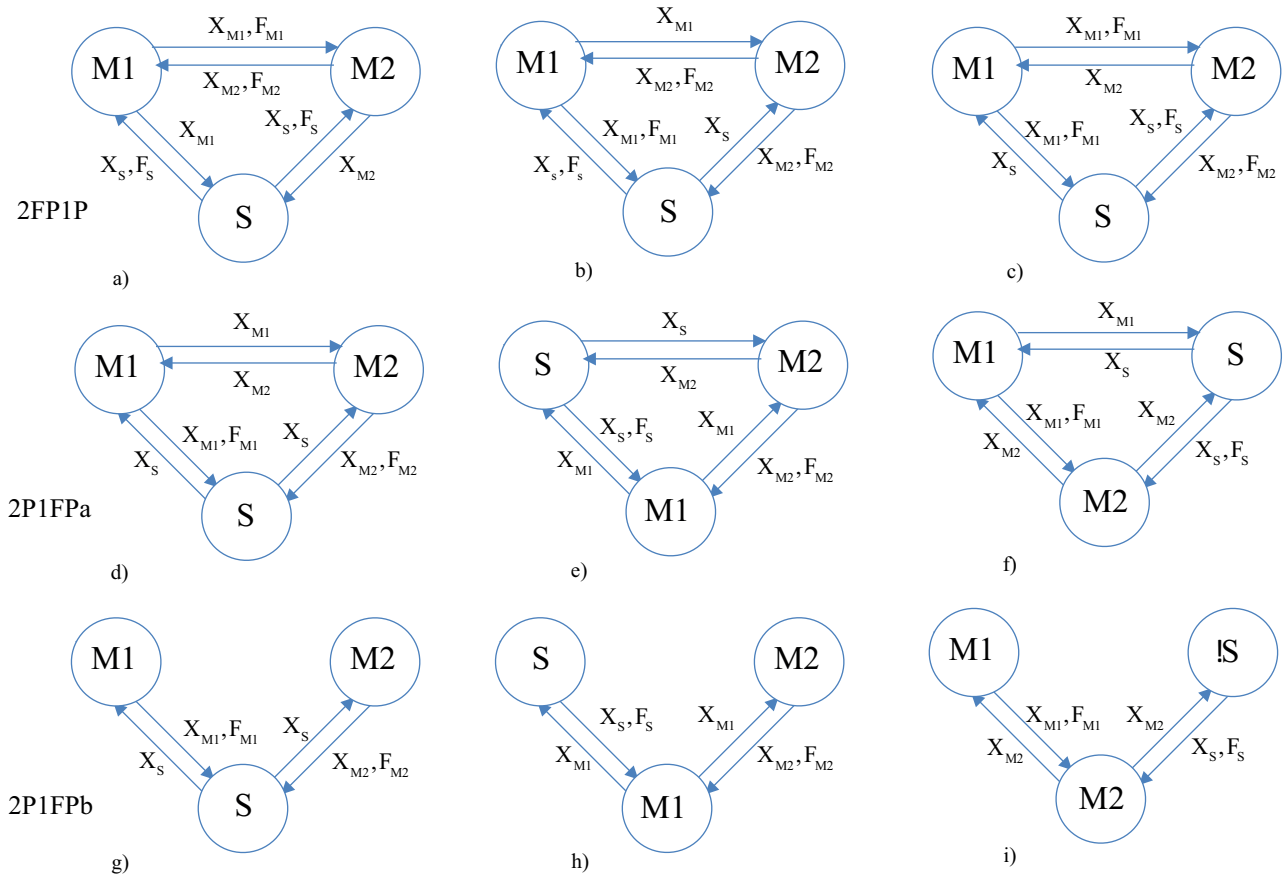

Figure 4. Possible three-channel communication architectures.

Here, $C_6^{m_1}$ and $C_6^{m_2}$, which are local force feedback channels of master 1 and master 2, are utilized for pure position control in master robots. Also, the master robots do not receive force information from the slave, and position or force information from each other. The slave robot on the other hand receives position and force information from both robots. All the local position controllers C_5 include damping injection terms b_{mi} and b_s. This architecture can also be easily scaled to N robots, where 1 robot (master or the slave) will be force/position-controlled and all the other robots are position-controlled. Next, stability analysis for this architecture is provided.

3. Stability analysis

In our analysis, it is assumed that human and environment exogenous input signals are in L_2 space. Signals $f(t)$ in this space satisfy: $\int_0^\infty |f(t)|^2\, dt < \infty$ and the L_2 norm of the signal is given as $||f||_2 = \left(\int_0^\infty |f(t)|^2\, dt\right)^{1/2}$. The extended L_2 space L_{2e} is the space of signals which satisfy $\int_0^T |f(t)|^2\, dt < \infty$, where T is finite. Assuming $L_{2e}(U)$ as input and $L_{2e}(Y)$ as output signal spaces and an input–output mapping S, S is finite-gain L_2-stable if it has a gain γ_2 which is finite for all $T \geq 0$ and if it is bounded as: $||S(u)||_2 \leq \gamma_2 ||u||_2 + \beta$, where β is a constant. A multivariable closed loop system in input–output form can be seen in Figure 5 and has the equations:

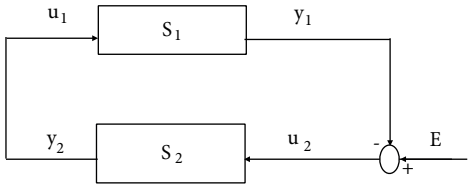

Figure 5. Input–output connected systems.

$$u_1 = y_2, \quad u_2 = E - y_1, \tag{23}$$

$$y_1 = S_1(u_1), \quad y_2 = S_2(u_2). \tag{24}$$

Here, S_1 and S_2 are MIMO subsystems. According to the small gain theorem, the input–output connected system will be L_2 input–output-stable if both S_1 and S_2 have finite gains $\gamma_2(S_1)$ and $\gamma_2(S_2)$, respectively and are stable, and also if the small gain condition is satisfied:

$$\gamma_2(S_1) \cdot \gamma_2(S_2) < 1. \tag{25}$$

This condition means that closed loop system has a small loop gain and is L_2-stable. In order to prove the L_2 stability of our proposed multilateral teleoperation system, the system has to be transformed into single-loop form as in Figure 5. Eqs. (5)–(9), (10)–(12), as well as (18)–(22) are used for modeling the environment and the operators and the system are transformed into input–output form as in Figure 5 and Eqs. (26) and (27).

In this paper, subsystems S_1 and S_2 in Figure 5 represent the local dynamics of the robots and the input–output connection is representative of the interconnection between the masters and slave. The subsystem S_1 contains the dynamics of the master robots and S_2 the slave robot. Due to the selection of 2P1FPb architecture, it becomes possible to combine the dynamics of master robots in S_1 as their dynamics are coupled only through the slave dynamics. According to the proposed three-channel architecture, the master systems are two single-input single-output systems, and the slave is a 2-input 2-output system. Since the dynamics for the masters are decoupled, they can be combined in the 2×2 S_1 subsystem and the slave dynamics is encapsulated by S_2, then we have:

$$S_1 = \begin{bmatrix} \frac{-Z_{m_1} e^{-T_{31}s} + C_p e^{-T_{31}s}}{m_{m_1} s^2 + b_{m1} s + C_p} & 0 \\ 0 & \frac{-Z_{m_2} e^{-T_{32}s} + C_p e^{-T_{32}s}}{m_{m_1} s^2 + b_{m2} s + C_p} \end{bmatrix}, \tag{26}$$

$$S_2 = \begin{bmatrix} \frac{C_p e^{-T_{13}s}}{m_s s^2 + b_s s + 2C_p + Z_s} & \frac{C_p e^{-T_{13}s}}{m_s s^2 + b_s s + 2C_p + Z_s} \\ \frac{C_p e^{-T_{23}s}}{m_s s^2 + b_s s + 2C_p + Z_s} & \frac{C_p e^{-T_{23}s}}{m_s s^2 + b_s s + 2C_p + Z_s} \end{bmatrix}. \tag{27}$$

Also, $E = F^*_{m1} e^{-T_{31}} s + F^*_{m2} e^{-T_{32s}} - F^*_s$ is an L_2 signal by definition. The L_2-induced gain of a subsystem is the H_∞ norm:

$$\gamma_2(S) = \sup_{w>0} \sigma_{max}(S(jw)), \tag{28}$$

$$\sigma_{max}(S(jw)) = \sqrt{\lambda_{max}\{S^*(jw)S(jw)\}}, \tag{29}$$

where $S^*(jw)$ is the conjugate transpose and λ are eigenvalues of $S(jw)$. We have for the first subsystem:

$$\sigma_{max}(S_1(jw)) = \quad max\Big\{\sqrt{(\frac{-Z_{m_1}e^{-T_{31}s}+C_pe^{-T_{31}s}}{m_{m_1}s^2+b_{m1}s+C_p})(\frac{-Z_{m_1}e^{-T_{31}s}+C_pe^{-T_{31}s}}{m_{m_1}s^2+b_{m1}s+C_p})^*}, \tag{30}$$
$$\sqrt{(\frac{-Z_{m_2}e^{-T_{32}s}+C_pe^{-T_{32}s}}{m_{m_2}s^2+b_{m2}s+C_p})(\frac{-Z_{m_2}e^{-T_{32}s}+C_pe^{-T_{32}s}}{m_{m_2}s^2+b_{m2}s+C_p})^*}\Big\}$$

and for the second subsystem:

$$\sigma_{max}(S_2(jw)) =$$
$$\sqrt{\frac{2C_pC_p^*e^{-T_{13}s}e^{T_{13}s}}{(m_ss^2+b_ss+2C_p+Z_s)(m_ss^2+b_ss+2C_p+Z_s)^*}+\frac{2C_pC_p^*e^{-T_{23}s}e^{T_{23}s}}{(m_ss^2+b_ss+2C_p+Z_s)(m_ss^2+b_ss+2C_p+Z_s)^*}}$$
$$=\sqrt{\frac{4C_pC_p^*}{(m_ss^2+b_ss+2C_p+Z_s)(m_ss^2+b_ss+2C_p+Z_s)^*}} \tag{31}$$

The small gain condition and L_2 stability conditions are satisfied if the individual subsystem gains can be designed to satisfy:

$$\gamma_2(S_1), \gamma_2(S_1) < 1, \tag{32}$$
$$\sup_{w>0}\sigma_{max}(S_1(jw)) < 1, \sup_{w>0}\sigma_{max}(S_2(jw)) < 1. \tag{33}$$

This gives us the following constraints for the first subsystem and therefore the master robots as a function of frequency ω:

$$((k_p-k_{zmi})^2+2(k_p-k_{zmi})m_{zmi}\omega^2+(k_v-b_{zmi})^2\omega^2+(m_{zmi}\omega^2)^2)/(k_p^2-2k_pm_{mi}\omega^2+$$
$$(k_v+b_{mi})^2\omega^2+(m_{mi}\omega^2)^2) < 1, \ \forall\omega > 0 \tag{34}$$

and the following constraint for the slave robot:

$$2(k_p^2+k_v^2\omega^2)/((2k_p+k_{ze})^2-2(2k_p+k_{ze})(m_s+m_{ze})\omega^2+(b_s+b_{ze}+2k_v)^2\omega^2+$$
$$((m_s+m_{ze})\omega^2)^2) < 1/2, \ \forall\omega > 0. \tag{35}$$

Controller parameters that can guarantee stability under all environmental impedance parameters can be determined by satisfying these constraints. Stability constraint in Eq. (34), for the master systems, can be divided into simpler inequalities by collecting the coefficients of the constant terms in the numerator and denominator and comparing them:

$$(k_p-k_{zmi})^2 < k_p^2, \tag{36}$$
$$k_p^2-2k_pk_{zmi}+k_{zmi}^2 < k_p^2, \tag{37}$$
$$k_{zmi}^2 < 2k_pk_{zmi}, \tag{38}$$
$$\frac{k_{zmi}}{2} < k_p. \tag{39}$$

Collecting and comparing the coefficients of the ω^2 terms while omitting the negative k_{zmi} term in the numerator:

$$(k_v - b_{zmi})^2 + 2k_p m_{zmi} < (k_v + b_{mi})^2 - 2k_p m_{mi}, \tag{40}$$

$$k_v^2 + b_{zmi}^2 - 2k_v b_{zmi} + 2k_p m_{zmi} < k_v^2 + 2k_v b_{mi} + b_{mi}^2 - 2k_p m_{mi}, \tag{41}$$

$$b_{zmi}^2 - 2k_v b_{zmi} + 2k_p m_{zmi} < 2k_v b_{mi} + b_{mi}^2 - 2k_p m_{mi}, \tag{42}$$

$$b_{zmi}^2 + 2k_p(m_{mi} + m_{zi}) < b_{mi}^2 + 2k_v b_{mi}. \tag{43}$$

Comparing the coefficients of ω^4 terms in the numerator and denominator:

$$m_{zmi} \leq m_{mi}. \tag{44}$$

By collecting the terms in a similar way for the slave in Eq. (35), it can be clearly seen that the condition is satisfied if the coefficients of the ω^2 terms in the numerator and denominator satisfy:

$$(b_s + b_{ze} + 2k_v)^2 - (4k_p + 2k_{ze})(m_s + m_{ze}) > 4k_v^2, \tag{45}$$

$$b_s^2 + b_{ze}^2 + 4k_v^2 + 2b_s b_{ze} + 4b_s k_v + 4k_v b_{ze} - (4k_p + 2k_{ze})(m_s + m_{ze}) > 4k_v^2. \tag{46}$$

Assuming that the environmental damping coefficient b_{ze} is 0 (worst case condition) we have:

$$b_s^2 + 4b_s k_v > (4k_p + 2k_{ze})(m_s + m_{ze}). \tag{47}$$

Together these constraints can be used to determine controller coefficients and can be summarized as:

$$k_p \geq k_{zmi}/2, \quad m_{mi} \geq m_{mzi}, \tag{48}$$

$$b_{mi}^2 + 2k_v b_{mi} > b_{zmi}^2 + 2(m_{mi} + m_{zi})k_p, \quad b_s^2 + 4k_v b_s > 2(2k_p + k_{ze})(m_s + m_{ze}). \tag{49}$$

It should be noted that these terms are conservative, as several simplifying assumptions and omissions have been made in the derivation. Furthermore, the individual subsystems are forced to satisfy the constraints in Eqs. (34) and (35), which adds to the conservatism. In actuality, one of the subsystems can have a larger gain but the product of the gains of the subsystems can still have a gain smaller than one. This implies that the obtained control parameters are not the boundary conditions for stability and hence provide a degree of robustness for variations in the parameters. Furthermore, in this paper, the damping coefficients b_{m1}, b_{m2}, and b_s will be chosen identical for transparency purposes, adding to the robustness of the system. m_{mi} terms can be adjusted with disturbance observers [25] if the robot has a smaller mass than that of the operator hand. The position controller gains should be selected greater than half the maximum master stiffness. With this controller, the system can be made L_2-stable independent of time delay for all environment parameters. In the next section, the transparency of the system under time delay will be discussed.

4. Transparency analysis

In order to quantify the performance of a teleoperation system, hybrid matrices are often utilized [5]. In bilateral teleoperation, the hybrid matrix is a two by two matrix that gives the relationship between master and slave

velocities/positions and master and slave forces in frequency domain. The hybrid matrix H and the ideal transparency conditions are given by:

$$\begin{bmatrix} F_m \\ -\dot{x}_s \end{bmatrix} = \underbrace{\begin{bmatrix} h_{11} & h_{12} \\ h_{21} & h_{22} \end{bmatrix}}_{H} \begin{bmatrix} \dot{x}_m \\ -F_m \end{bmatrix}, \quad H_{ideal} = \underbrace{\begin{bmatrix} 0 & -1 \\ -1 & 0 \end{bmatrix}}, \tag{50}$$

where F_m, F_s, x_m, and x_s are the master and slave forces and master and slave positions, respectively. These conditions are ideal and cannot be exactly attained due to controller bandwidth constraints, but the more these relations are approximated, the better the transparency becomes. In the case of multilateral teleoperation, due to the constraint in Eq. (1), the hybrid matrices become singular and cannot be employed. Some papers have utilized impedance matrices [27]; however, these matrices do not provide an intuitive understanding for the performance of the multilateral teleoperation system as defined by Eqs. (1) and (2). Therefore, in order to visualize these equations, the use of inverse hybrid matrices is proposed. The inverse hybrid matrices G and the ideal transparency conditions are given as:

$$\begin{bmatrix} \dot{x}_{m1} \\ \dot{x}_{m2} \\ -F_s \end{bmatrix} = \underbrace{\begin{bmatrix} g_{11} & g_{12} & g_{13} \\ g_{21} & g_{22} & g_{23} \\ g_{31} & g_{32} & g_{33} \end{bmatrix}}_{G} \begin{bmatrix} F_{m1} \\ F_{m2} \\ -\dot{x}_s \end{bmatrix}, \quad G_{ideal} = \begin{bmatrix} 0 & 0 & -1 \\ 0 & 0 & -1 \\ -1 & -1 & 0 \end{bmatrix}. \tag{51}$$

By plugging in the selected channel parameters in the robot dynamics in Eqs. (5)–(12), the elements of the inverse hybrid matrices under time delay for various Lawrence (two-, three-, or four-channel)-based multilateral architectures can be solved. The inverse hybrid matrix elements are found as:

$$\begin{aligned} g_{11} = \quad & D^{-1}(-Z^{cm2}(C_6^{m1}C_6^s - C_4^{m1}C_3^s e^{-s(T_{13}+T_{31})}) - C_1^{m1}(C_3^{m2}C_6^s e^{-T_{21}s} - C_4^{m2}C_3^s e^{-s(T_{23}+T_{31})})e^{-T_{12}s} \\ & -C_2^s(C_4^{m2}C_6^{m1}e^{-T_{23}s} - C_3^{m2}C_4^{m1}e^{-s(T_{13}+T_{21})})e^{-T_{32}s}), \end{aligned} \tag{52}$$

$$\begin{aligned} g_{12} = \quad & D^{-1}(C_4^{m1}(Z^{cm2}C_4^s + C_6^{m2}C_2^s)e^{-s(T_{13}+T_{32})} - C_6^s(C_3^{m1}Z^{cm2} + C_1^{m1}C_6^{m2})e^{-T_{12}s} \\ & +C_4^{m2}(C_1^{m1}C_4^s - C_3^{m1}C_2^s)e^{-s(T_{12}+T_{23}+T_{32})}), \end{aligned} \tag{53}$$

$$\begin{aligned} g_{13} = \quad & D^{-1}(-Z^{cm2}(C_2^{m1}C_6^s + C_4^{m1}Z^{cs})e^{-T_{13}s} - C_1^{m1}(C_4^{m2}Z^{cs} + C_2^{m2}C_6^s)e^{-s(T_{12}+T_{23})} \\ & -C_2^s(C_2^{m1}C_4^{m2} - C_2^{m2}C_4^{m1})e^{-s(T_{13}+T_{23}+T_{32})}), \end{aligned} \tag{54}$$

$$\begin{aligned} g_{21} = \quad & D^{-1}(C_4^{m2}(Z^{cm1}C_3^s + C_6^{m1}C_1^s)e^{-s(T_{23}+T_{31})} - C_6^s(C_1^{m2}C_6^{m1} + C_3^{m2}Z^{cm1})e^{-T_{21}s} \\ & +C_4^{m1}(C_1^{m2}C_3^s - C_3^{m2}C_1^s)e^{-s(T_{13}+T_{21}+T_{31})}), \end{aligned} \tag{55}$$

$$\tag{56}$$

$$g_{22} = D^{-1}(-Z^{cm1}(C_6^{m2}C_6^s - C_4^{m2}C_4^s e^{-s(T_{23}+T_{32})}) - C_1^{m2}(C_3^{m1}C_6^s e^{-T_{12}s} - C_4^{m1}C_4^s e^{-s(T_{13}+T_{32})})e^{-T_{21}s}$$
$$-C_1^s(C_4^{m1}C_6^{m2}e^{-T_{13}s} - C_3^{m1}C_4^{m2}e^{-s(T_{12}+T_{23})})e^{-T_{31}s}), \quad (57)$$

$$g_{23} = D^{-1}(-Z^{cm1}(C_2^{m2}C_6^s + C_4^{m2}Z^{cs})e^{-T_{23}s} - C_1^{m2}(C_4^{m1}Z^{cs} + C_2^{m1}C_6^s)e^{-s(T_{13}+T_{21})}$$
$$-C_1^s(C_2^{m2}C_4^{m1} - C_2^{m1}C_4^{m2})e^{-s(T_{13}+T_{23}+T_{31})}), \quad (58)$$

$$g_{31} = D^{-1}(-Z^{cm2}(C_6^{m1}C_1^s + C_3^s Z^{cm1})e^{-T_{31}s} - C_2^s(C_3^{m2}Z^{cm1} + C_1^{m2}C_6^{m1})e^{-s(T_{21}+T_{32})}$$
$$-C_1^{m1}(C_3^{m2}C_1^s - C_1^{m2}C_3^s)e^{-s(T_{12}+T_{21}+T_{31})}), \quad (59)$$

$$g_{32} = D^{-1}(-Z^{cm1}(C_6^{m2}C_2^s + C_4^s Z^{cm2})e^{-T_{32}s} - C_1^s(C_3^{m1}Z^{cm2} + C_1^{m1}C_6^{m2})e^{-s(T_{12}+T_{31})}$$
$$-C_1^{m2}(C_3^{m1}C_2^s - C_1^{m1}C_4^s)e^{-s(T_{12}+T_{21}+T_{32})}), \quad (60)$$

$$g_{33} = D^{-1}(Z^{cm1}Z^{cm2}Z^{cs} - C_2^{m1}C_1^s Z^{cm2}e^{-s(T_{13}+T_{31})} - C_1^{m1}(C_2^{m2}C_1^s e^{-s(T_{23}+T_{31})} + C_1^{m2}Z^{cs}e^{-sT_{21}})e^{-T_{12}s}$$
$$-C_2^s(C_1^{m2}C_2^{m1}e^{-s(T_{13}+T_{21})} + C_2^{m2}Z^{cm1}e^{-sT_{23}})e^{-T_{32}s}), \quad (61)$$

$$D = C_4^{m1}C_1^s Z^{cm2}e^{-s(T_{13}+T_{31})} + C_4^{m2}C_2^s Z^{cm1}e^{-s(T_{23}+T_{32})} + C_6^s(Z^{cm2}Z^{cm1} - C_1^{m1}C_1^{m2})e^{-s(T_{12}+T_{21})}$$
$$+C_1^{m1}C_4^{m2}C_1^s e^{-s(T_{12}+T_{23}+T_{31})} + C_1^{m2}C_4^{m1}C_2^s e^{-s(T_{13}+T_{21}+T_{32})}, \quad (62)$$

where

$$Z^{cm1} = C_5^{m1} + Z_{m1}, Z^{cm2} = C_5^{m2} + Z_{m2}, Z^{cs} = C_5^{m2} + Z_s. \quad (63)$$

The frequency response of these elements are plotted for performance analysis. Figure 6 shows the frequency domain magnitude plots of the inverse hybrid matrix elements for the two-channel, four-channel, and the proposed three-channel (2P1FPa, Figure 4g) trilateral architectures with 0.2-s time delay on each channel, with similar parameters of $k_p = 900, k_v = 60, b_{mi} = b_s = 20, m_{mi} = m_s = 0.2$. These plots give an intuitive transparency comparison between these architectures. The magnitude plots show that while the three-channel architecture can achieve the ideal 0 value for all frequencies (g_{11}, g_{12}, g_{21}, and g_{22}), the four-channel and two-channel architectures cannot due to time delay. On the other hand, g_{13}, g_{23}, g_{31}, and g_{32} values should be ideally equal to one (0dB). The bode magnitude plots for these elements show that two-channel and four-channel architectures suffer from large and fast variations in magnitude along the frequency domain due to time delay, whereas the proposed three-channel architecture is unaffected by this. g_{31} and g_{32} channels show the force reflection relationship in the system more specifically, and perfect force reflection is achieved in the whole frequency range. It can be seen that the two-channel PP architecture response crosses the bandwidth threshold of –3 dB at 3.887 rads/s and while showing large variations, is mostly below the threshold value. While the four-channel architecture response also oscillates and crosses the –3 dB line, mostly it is above the –3 dB line and as frequency increases, it settles to 0 dB. Neither of these responses are ideal in terms of transparency. In g_{13} and g_{23}, position relations are given, and the three-channel system has a second order system response. The bandwidth and damping ratio of this response can be designed by adjusting the k_p, k_v, and b_{mi}, b_s terms in the controller. The bandwidth for the position response of the two-channel architecture is seen to be at 192.4 rads/s. The two-channel and four-channel architectures have similar responses to their force responses with large variations over the frequency range. A method to increase the bandwidth of the position channels was proposed by Lawrence [6] in the form of acceleration information exchange among the robots, but that approach has been omitted due to difficulties in implementation. Finally, the g_{33} element shows the impedance felt by

the user during teleoperation. It can be seen that all the controllers behave similarly in this regard. For low frequencies, while moving the robot, the user feels a constant damping determined by the damping injection terms that stabilize the system. As a result, the larger the damping is, the slower the system will be. This is a trade-off between stability and transparency under time delay. It should be noted that all other three-channel controllers in Figure 4, except a, b, and c, have similar responses but they have been omitted for brevity.

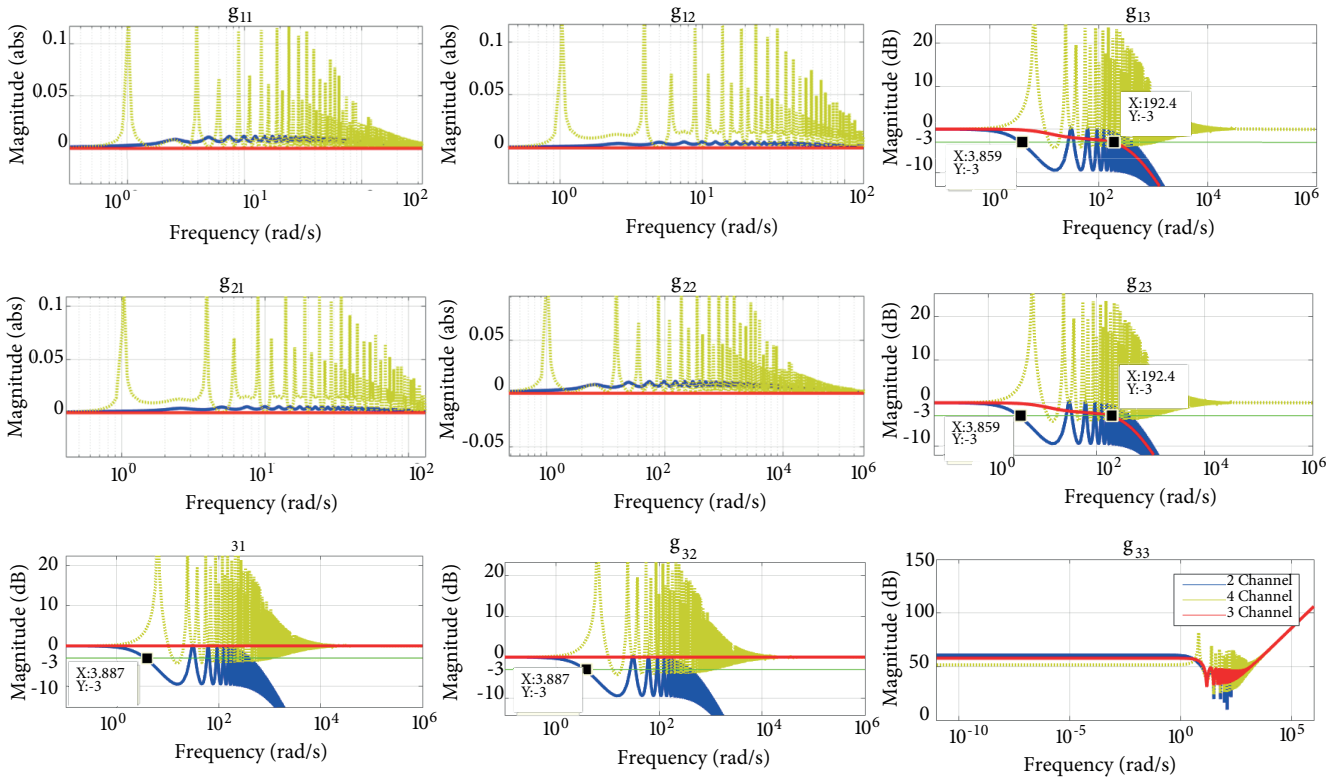

Figure 6. Transparency plots.

5. Experiment results

Validity of the analytical and computational results was confirmed with experiments. The trilateral teleoperation system was composed of three linear BLDC motors Dunkermotoren STA1116 as seen in Figure 7. The motors were connected to a computer through two DAQ cards (PCIe-6321, National Instruments, Austin, TX, USA), and the computer runs the control algorithm in real time in MATLAB Simulink with a sampling time of 1 ms. High-resolution hall sensors integrated to the motors are utilized for position measurement and disturbance observers are utilized for disturbance compensation and force estimation [28, 29]. Two-channel, four-channel, and the proposed three-channel architecture (Figure 4g) have been implemented as control laws. The proposed controller was tested with time delays up to 0.5 s among each robot and the system was stable as expected due to the delay-independent stability of the proposed controller. However, as in any teleoperation system, the transparency deteriorates as a result of the increase in time delay, and the system response becomes slower. This paper presents the case where all of the time delays are identical and 0.2 s.

In the experiments, as can be seen in Figure 7, two operators move two master motors' shafts and the slave motor follows their motion and then contacts a wooden surface. This period without contact with

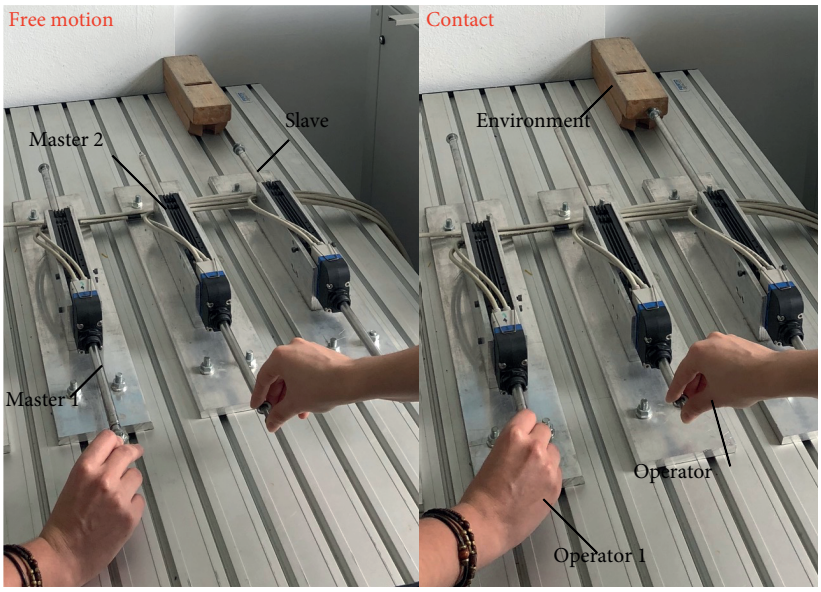

Figure 7. Trilateral teleoperation experiment setup.

the environment is called free-motion. During contact period, the master operators apply varying amounts of force on the master motors. Then the operators move the shafts backwards, the free motion and contact is repeated once more. The goal in these experiments was to see that positions track each other under all circumstances and the sum of the force measurements is 0. The impedance of the motors used in the experiment setup is $Z_{m1}(s) = Z_{m2}(s) = Z_s(s) = m_{m1}s = m_{m2}s = m_s s = 0.2s$ as the shaft masses are 0.2 kg. The motor dynamics can simply be modeled by a mass with the use of disturbance observers [25]. Furthermore since high-frequency current control at 15 kHz is performed by the motor drivers, the electrical dynamics is negligible. By using the human impedance assumption of $48/s + 4.5 + 0.2s$ [25, 30] and wooden surface stiffness assumption of $k_{ze} = 10000N/m$[25], the controller parameters of the three-channel controller were selected as $k_p = 900N/m, k_v = 60Ns/m, b_{mi} = b_s = 20Ns/m$ according to Eqs. (48) and (49). Four-channel teleoperation architecture is also utilized with the same controller gains. Two-channel controller also has the same PD gains but does not utilize damping injection. It should be noted that the human and environmental impedances have been used as design guidelines and are not assumed to be exact. The damping injection terms selected here are greater than actual boundary stability conditions as explained in Section 3 and provide robustness to variations. A more exact robust stability analysis can be performed as in [25] to a varying set of environment/human impedances, but is not the focus of this paper.

The experiment results show that, while all controllers can guarantee stable teleoperation under time delay, two-channel controllers (Figure 8) have large steady-state errors during contact (8–16 s, 23–30 s). Free-motion position tracking is acceptable. Four-channel controller (Figure 9) eliminates steady-state errors during contact seen in two-channel control but has overshooting behavior in both position and force reflection during contact (6–16 s, 23–33 s), which feels like a fictitious recoil motion to the operators and deteriorates transparency. On the other hand, three-channel controller (Figure 9) achieves position tracking and force reflection even during contact (8–20 s, 32–50 s) without overshoot, allowing phase lag between masters and the slave and satisfying delayed transparency conditions [9]. It can also be seen in Figure 10 that the force response also has higher frequency components consistent with the transparency and bandwidth analysis provided in Figure 6.

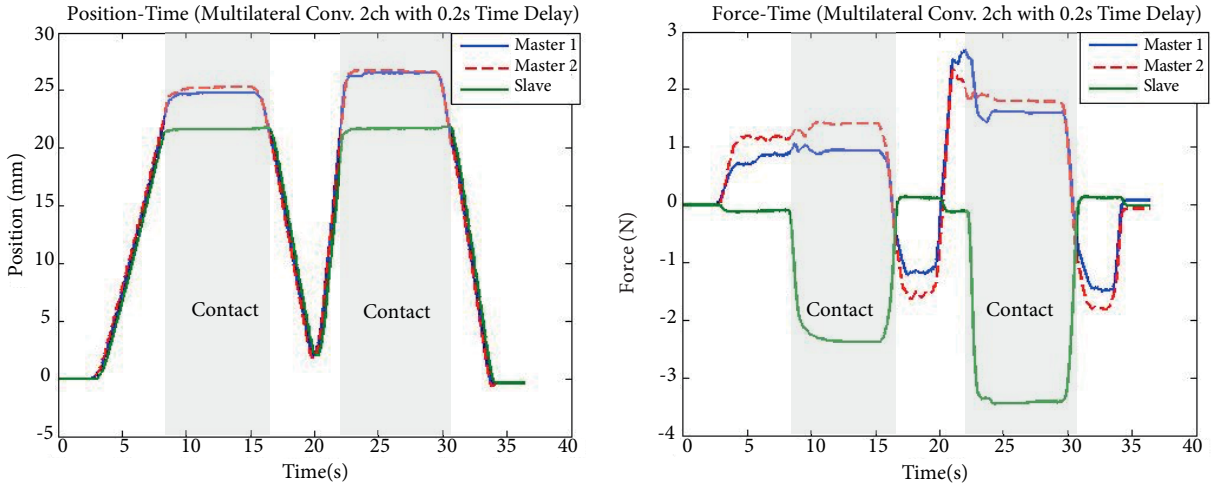

(a) Position Response (b) Force Response

Figure 8. Performance of two-channel multilateral teleoperation with 200 ms delay between each robot.

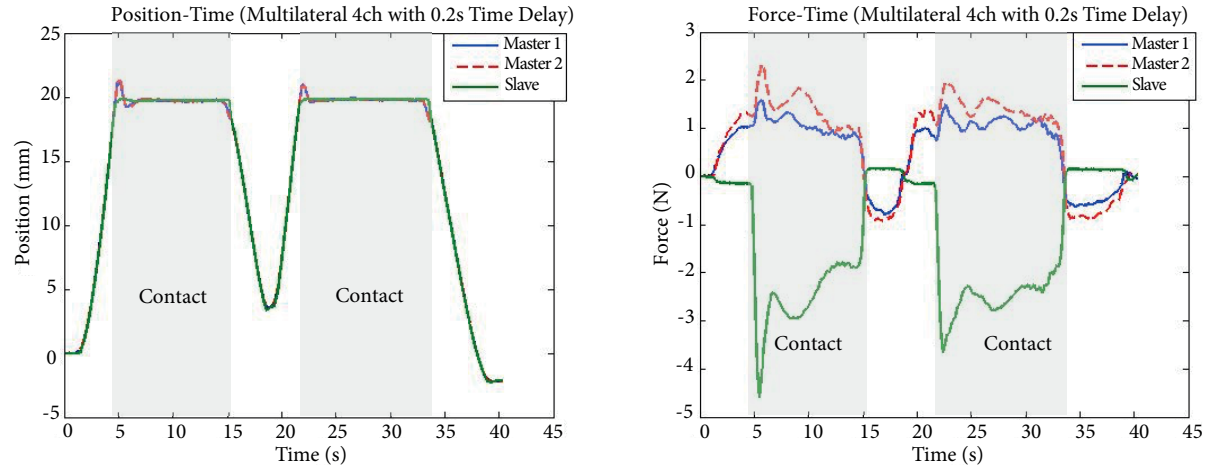

(a) Position Response (b) Force Response

Figure 9. Performance of four-channel multilateral teleoperation with 200 ms delay between each robot.

It can be seen that the proposed three-channel architecture can achieve stable teleoperation under time delay. The proposed controller has zero steady-state error in position tracking during contact just like the four-channel controller. However, transient behavior of the three-channel architecture is superior to the four-channel architecture as there is no overshoot during contact. The two-channel architecture, on the other hand, is characterized by the large steady-state error during contact. All architectures can achieve force reflection; however, the proposed three-channel controller responses also show higher frequency components during contact. These results confirm the validity of the proposed method and analysis provided in the previous sections.

6. Conclusion

This paper extended the three-channel control architecture to multilateral systems and proposed modifications for improvements in transparency and stability under time delay. With the extension of three-channel architecture to multilateral control, it was shown with experiments and numerical analysis that better transparency

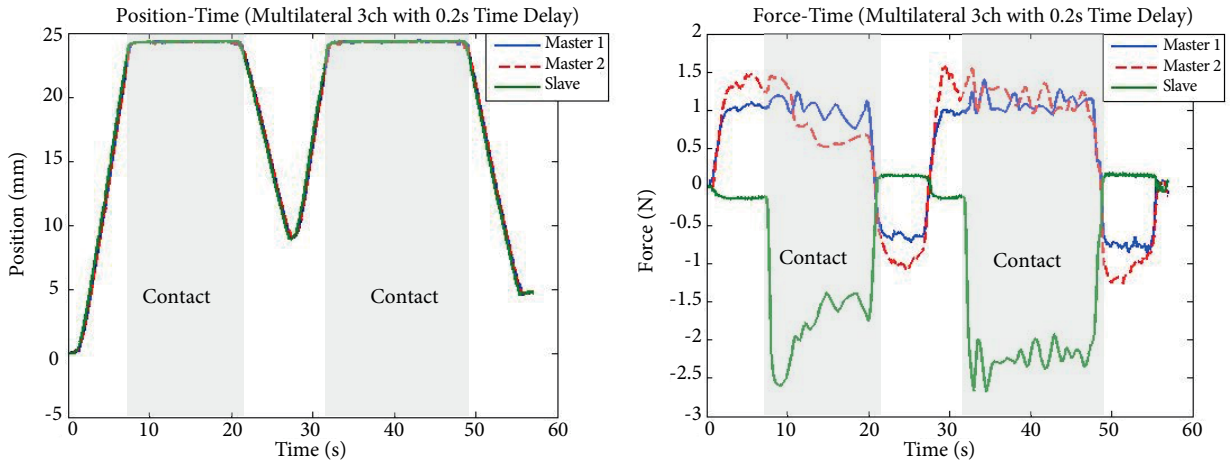

(a) Position Response (b) Force Response

Figure 10. Performance of proposed three-channel multilateral teleoperation with 200 ms delay between each robot.

can be achieved compared to two-channel and four-channel-based multilateral teleoperation architectures under constant time delay. One of the most difficult problems in developing controllers for multilateral systems, especially under time delay, is in the analysis of stability with multiple force–position channels. An L_2 stability analysis method was developed specifically for the 3-channel architecture proposed in this paper, and it was shown that damping injection can be utilized in conjunction with three-channel architecture to guarantee delay-independent stability, by taking environmental impedances into consideration. Another problem was in the analysis of transparency; although there are known transparency analysis techniques in bilateral teleoperation, these are not directly applicable to multilateral teleoperation. For this reason, in this paper, inverse hybrid matrices were utilized instead of hybrid matrices. Even in the special case of three robot teleoperation, there are 9 matrix elements and derivation of these elements becomes very involved. These matrices were utilized to compare the transparency of the proposed and existing Lawrence architectures under time delay. The design and analysis approach used here can be applied to other possible bilateral Lawrence architectures in multilateral teleoperation with N robots. Furthermore, the method can also be extended to accommodate different dominance ratios among masters.

References

[1] Hagn U, Konietschke R, Tobergte A, Nickl M, Joerg S, Kuebler B, Passig G, Groeger M, Froehlich F, Seibold U et al. DLR MiroSurge: a versatile system for research in endoscopic telesurgery. Int J CARS 2010; 5: 183-193.

[2] Atashzar SF, Polushin IG, Patel RV. Networked teleoperation with non-passive environment: application to tele-rehabilitation. In: 2012 IEEE/RSJ International Conference on Intelligent Robots and Systems(IROS); 7-12 October 2012; Vilamoura, Portugal: IEEE. pp. 5125-5130.

[3] Kim J, Ahn B, Kim Y, Kim J. Inclusion detection with haptic-palpation system for medical telediagnosis. In: 2009 Annual Conference of the IEEE Engineering in Medicine and Biology; 3-6 September 2009; Minneapolis, Minnesota, USA: IEEE. pp. 4595-4598.

[4] Anderson RJ, Spong MW. Bilateral control of teleoperators with time delay. IEEE Trans Autom Control 1989; 34: 494-501.

[5] Hannaford B. A design framework for teleoperators with kinesthetic feedback. IEEE Trans Robot Autom 1989; 5: 426-434.

[6] Lawrence DA. Stability and transparency in bilateral teleoperation. IEEE Trans Robot Autom 1993; 9: 624-637.

[7] Alfi A, Bakhshi A, Yousefi M, Talebi HA. Design and implementation of robust-fixed structure controller for telerobotic systems. J Intell Robot Syst 2016; 83: 253-269.

[8] Hastrudi-Zaad K, Salcudean SE. On the use of local force feedback for transparent teleoperation. In: 1999 IEEE International Conference on Robotics and Automation; 10-15 May 1999; Detroit, MI, USA: IEEE. pp. 1863-1869.

[9] Hashtrudi-Zaad K, Salcudean SE. Transparency in time-delayed systems and the effect of local force feedback for transparent teleoperation. IEEE Trans Robot Autom 2002; 18: 108-114.

[10] Tumerdem U, Ohnishi K. L_2 stability analysis of four channel teleoperation and experiments under varying time delay. In: 2010 IEEE International Workshop on Advanced Motion Control; 21-24 March 2010; Nagaoka, Japan: IEEE. pp. 643-648.

[11] Shahbazi M, Atashzar SF, Patel R. A systematic review of multilateral teleoperation systems. IEEE Trans Haptics 2018; 11: 338-356.

[12] Katsura S, Ohnishi K. A realization of haptic training system by multilateral control. IEEE Trans Ind Electron 2006; 53: 1935-1942.

[13] Khademian B, Hashtrudi-Zaad K. A robust multilateral shared controller for dual-user teleoperation systems. In: 2008 Canadian Conference on Electrical and Computer Engineering; 4-7 May 2008; Niagara Falls, Canada: IEEE. pp. 1871-1876.

[14] Mendez V, Tavakoli M. A passivity criterion for n-port multilateral haptic systems. In: 49th IEEE Conference on Decision and Control; 15-17 December 2010; Atlanta, GA, USA: IEEE. pp. 274-279.

[15] Shahbazi M, Talebi HA, Yazdanpanah MJ. A control architecture for dual user teleoperation with unknown time delays: a sliding mode approach. In: 2010 IEEE/ASME International Conference on Advanced Intelligent Mechatronics; 6-9 July 2010; Montreal, Canada: IEEE. pp. 1221-1226.

[16] Takahiro K, Yokokohji Y. Multilateral teleoperation control over time-delayed computer networks using wave variables. In: 2012 IEEE Haptics Symposium; March 4-7 2012; Vancouver, Canada: IEEE. pp. 125-131.

[17] Van Quang H, Ryu JH. Stable multilateral teleoperation with time domain passivity approach. In: 2013 IEEE/RSJ International Conference on Intelligent Robots and Systems; November 3-7 2013; Tokyo, Japan: IEEE. pp. 5890-5895.

[18] Huang K, Lee D. Consensus-based peer-to-peer control architecture for multiuser haptic interaction over the internet. IEEE Trans Robot 2013; 29: 417-31.

[19] Sun D, Naghdy F, Du H. Stability control of force-reflected nonlinear multilateral teleoperation system under time-varying delays. J Sensors 2016; 2016: 4316024.

[20] Chen Z, Pan YJ, Gu J. Integrated adaptive robust control for multilateral teleoperation systems under arbitrary time delays. Int J Robust Nonlin 2016; 26: 2708-2728.

[21] Ghorbanian A, Rezaei SM, Khoogar AR, Zareinejad M, Baghestan K. A novel control framework for nonlinear time-delayed dual-master/single-slave teleoperation. ISA Trans 2013; 52: 268-277.

[22] Razi K, Hashtrudi-Zaad K. Analysis of coupled stability in multilateral dual-user teleoperation systems. IEEE Trans Robot 2014; 30: 631-641.

[23] Li J, Tavakoli M, Mendez V, Huang Q. Passivity and absolute stability analyses of trilateral haptic collaborative systems. J Intell Robot Syst 2015; 78: 3-20.

[24] Hashtrudi-Zaad K, Salcudean SE. Analysis of control architectures for teleoperation systems with impedance/admittance master and slave manipulators. Int J Robotics Res 2001; 20: 419-445.

[25] Tumerdem U. Multilateral teleoperation under asymmetric time delays: L_2 stability and robustness. Int J Adv Robot Syst 2017; 14: 1729881417710148.

[26] Li J, Tavakoli M, Huang Q. Absolute stability of a class of trilateral haptic systems. IEEE Trans Haptics 2014; 7: 301-310.

[27] Shamaei K, Kim LH, Okamura AM. Design and evaluation of a trilateral shared-control architecture for teleoperated training robots. In: 2015 Annual International Conference of the Engineering in Medicine and Biology Society (EMBC); 25-29 August 2015; Milan, Italy: IEEE. pp. 4887-4893.

[28] Ohnishi K, Shibata M, Murakami T. Motion control for advanced mechatronics. IEEE/ASME Trans Mechatronics 1996; 1: 56-67.

[29] Murakami T, Yu F, Ohnishi K. Torque sensorless control in multidegree-of-freedom manipulator. IEEE Trans Ind Electron 1993; 40: 259-265.

[30] Speich JE, Shao L, Goldfarb M. Modeling the human hand as it interacts with a telemanipulation system. Mechatronics 2005; 15: 1127-1142.